

Proton transfer pathways in an aspartate-water cluster sampled by a network of discrete states.

Marco Reidelbach, Fridtjof Betz, Raquel Maya Mäusle¹, Petra Imhof^{1,*}

*Institute for Theoretical Physics
Freie Universität Berlin
Arnimallee 14
14195 Berlin
Germany*

Introduction

Proton transfer reactions are ubiquitous processes in chemistry such as acid-base reactions, and in biology, e.g. the light activated proton pumping of bacteriorhodopsin [1], the oxidative phosphorylation to produce adenosine triphosphate (ATP) in the respiratory chain [2, 3], or the photosynthetic water oxidation [4, 5]. Proton transfer is also crucial for bacterial motions [6], the human immune response [7], and antibiotics as gramicidin [8]. Insights into the mechanisms of these reactions could be beneficial to the design of fuel cells [9] or bioprotonic devices [10].

In 1806, Grotthus proposed a mechanism for the electrical decomposition of water, stating that in an electromotive apparatus only water molecules at the tip of the conducting wires are decomposed, while all intermediate water molecules, although collectively changing their composing principles, still remain to be water [11]. Subsequently, conceptual models to understand the properties of water and its ions were developed in the early 20th century [12, 13]. Detailed insight into the proton transfer mechanism, however, was only gained about 50 years later, when *ab initio* molecular dynamics (aiMD) simulations [14, 15, 16, 17] as well as the force-field based empirical valence bond approach [18, 19, 20] were applied. The essence of all these investigations is today known as the Grotthus mechanism, proclaiming that protons “hop” step-wise between neighbouring water molecules by exchanging covalent and hydrogen bonds connecting the proton to the donor or acceptor oxygen respectively [21, 22]. Each of these “hops” has to be followed by a reorganisation of the water molecules surrounding the proton-receiving water molecule, resulting in a 1–2 ps time scale for a single proton transfer step. Furthermore, according to Onsager the proton

*Corresponding author

Email address: `petra.imhof@fu-berlin.de` (Petra Imhof)

donor or acceptor does not have to be a water molecule, but could in principle be a polar (titratable) amino acid residue (e.g. aspartate) of a protein [23].

An alternative, rather coherent proton transfer mechanism, was suggested by Eigen in 1964 [24]. Here, protons could de-localise over extended water chains, subsequently called proton wires by Nagle and Morowitz [25], involving several simultaneous proton “hops”. Such mechanisms were indeed observed in linear water chains inside channels of proton conducting proteins [26] or carbon nanotubes [27, 28]. Furthermore, spectroscopic experiments concerning acid-base reactions in water and ice seem to indicate the formation of transient proton wires, which allow fast proton transfer reactions [29, 30]. Rearrangement of a second solvation shell facilitating proton transfer has also been observed in network analyses of proton transfer simulations by multi-state empirical valence bond molecular dynamics simulations [31]. Using aiMD Parrinello and coworkers [32] recently investigated the neutralisation of hydronium and hydroxide ions in water, revealing a collective compression and concerted motion of the proton wire connecting both ions. Furthermore, they suggested that proton transfer in water is a combination of active periods, during which the charge is translocated by concerted motions along proton wires, thereby covering 6–8 Å on a sub-picosecond timescale, and resting periods, in which the protons only “hop” Grothaus-like to the next water molecule [33].

The current investigations of proton transfer reactions in solution or in proteins often struggle with the sheer complexity of the problem, i.e. spatially, due to the highly connected hydrogen bond networks in water, as well as temporal, due to different time scales necessary for proton transfer events along proton wires or single Grothaus-like hops. To circumvent the need for a full quantum mechanically (QM) treatment of the whole system, methods have been developed that estimate the probability for a proton transfer between a donor and acceptor pair during an otherwise classical molecular dynamics simulation and either switch to the new protonation state [34], use multi-state valence-bond approaches [35, 36, 18] or the adjustment of the QM subsystem “on-the-fly” to enable computation of the proton transfer step [37]. Enhancing simulations by “driving” an excess proton can overcome the time scale problem but introduces a bias in the proton transfer pathway. For an unbiased understanding of proton transfer events, sampling of as many pathways as possible with as little pre-selection of pathways (or reaction coordinates) is, however, desirable.

This can be realised by sampling discrete proton transfer pathways between a given pair of end states on a potential energy surface. The discrete path sampling technique was introduced by Wales and coworkers [38, 39] and generates a large number of local minima and transition states between them, resulting in a network of connected pathways. A similar method is the Transition Network approach proposed by Noe *et al* [40]. The minima used to construct a network can be generated by direct sampling of points on a high-dimensional grid, spanned by either the Cartesian atomic coordinates or internal degrees of freedom of the polyatomic molecular system under investigation. That way, the sampling does not suffer from barriers that are unlikely to be overcome in e.g. a molecular dynamics simulation or the too low acceptance ratio of energetically

not favourable structures in Monte-Carlo methods. The difficulty with direct sampling is, however, the large number of minima and transitions that exist on a complex energy surface.

In this work, we therefore employ a combination of direct sampling for degrees of freedom that generate only a low number of states and are likely separated by substantial energy barriers, and molecular dynamics (MD) simulations based sampling for degrees of freedom that can result in a large number of states which are, however, connected by barriers that can be easily overcome. The combination of all states thus sampled and their connections constitutes the transition network on which the energetically most favourable proton transfer pathways are then determined.

In order to validate this combination approach we focus here on a small system (see Methods section) that can be understood as a model for water-filled protein channels and hydrogen-bonded networks in proteins. Such networks are found in e.g. Photosystem II [41], Cytochrome c oxidase [42, 43], or gramicidin-like channels [44, 8, 45]. The highly connected hydrogen bond networks in these systems render direct sampling unfeasible due to the prohibitive large number of states to consider. Many of those states, however, are energetically not favourable and therefore irrelevant for the determination of the most probable proton transfer pathways. To explore a large number of pathways so as to reflect the high diversity of proteins, it is important to sample many energetically accessible routes. The transition networks constructed from combined sampling, as presented in this work, allow an efficient and comprehensive sampling of such proton transfer pathways that can be easily applied to more complex protein environments.

1. Methods

Proton transfer pathways were calculated for a model system consisting of thirteen water molecules embedded in a cylinder, one excess proton, and two aspartate-like molecules at either end of the cylinder that can be understood as a small model system for water-filled protein channels. The aspartate-like molecules consist of a carboxyl group, representing the side chain of aspartate amino acids, and a bulky *t*-butyl-“backbone”, forming the top and bottom of a cylinder that was kept stationary in all simulations. The walls of the cylinder were modelled by a harmonic potential, setting on at 3.0 Å away from the cylindrical axis with a force constant of 500 kcal/mol/Å².

Two configurations with the excess proton located on either of the two aspartate mimics, were prepared as reactant and product state, i.e. end-states of the overall proton transfer reaction (see Fig. 1).

A transition network has the structure of a weighted, undirected graph. To construct the transition network for sampling proton transfer pathways, nodes were generated from initial structures, different in protonation state, dihedral conformation of the aspartate mimics, and water positions and orientations. To this end, two approaches were combined.

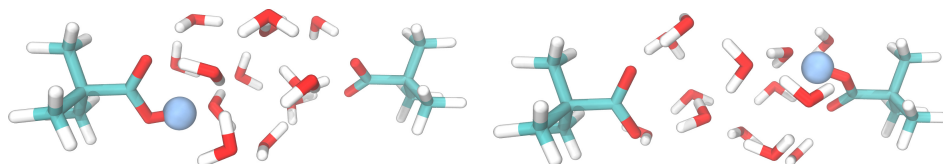


Figure 1: Model system for calculating proton transfer pathways, left: reactant, right: product. The blue sphere highlights the net change in protonation state.

In the first, direct sampling approach, protonation states were sampled by placing the excess proton on either of the water molecules or on the carboxyl groups of the aspartate mimics, resulting in 17 different protonation states. For each of these structures, the side chain dihedral angle of the aspartate mimics was varied with a step size of 45 degrees.

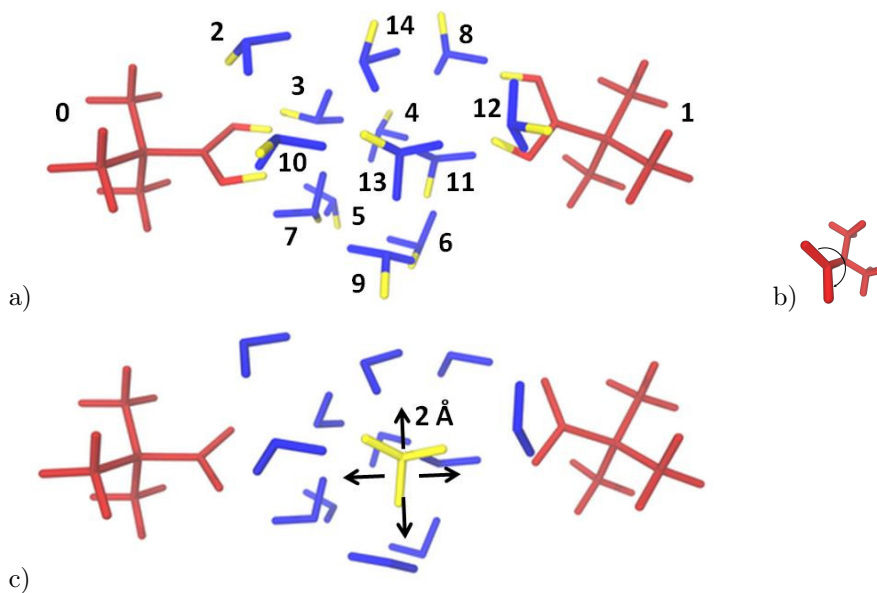


Figure 2: Degrees of freedom used in the direct sampling. a) Positions of an excess proton, highlighted in yellow, and numbering of the molecules. b) Aspartate side chain dihedral angle. c) Position of the excess-proton carrying water molecules (yellow).

In the second approach, the set of configurations generated by this direct sampling was augmented by samples taken from short (1 ns) classical MD simulations, carried out for the thirteen different water protonation states (for details see supplementary information). Snapshots were saved at 1 ps intervals, thereby generating 1000 configurations per water protonation state.

In an additional control, we applied direct sampling of side chain rotations, proton positions, and the position of the water molecule, carrying the excess proton. For the latter the respective water molecule was displaced by 2 Å forward

and backward, respectively, in all three directions of Cartesian space.

All configurations were then subjected to an energy minimisation with a convergence criterion of 0.001 kcal/mol/Å using the semi-empirical OM2 method [46] as energy function for QM optimisations. An evaluation of the OM2 method for computation of proton transfer along water molecules between two aspartate side chains is provided as supplementary information.

After minimisation, the optimised geometries were assigned to a network node, i.e. a discrete state. The assignment was based on the dihedral angle of the carboxylic side chains, the protonation state, i.e. the location of the excess proton on either a water molecule or an aspartate mimic, and a “water pattern”, characterised by the displacement and rotation of water molecules with the reactant state as reference. Note that also proton holes can be identified in the assignment but do not occur in the nodes of the present transition networks.

Assigned nodes are labelled as SC0.SC1.Wi.P. Here SC0 and SC1 correspond to the number of dihedral steps of the side chain of molecule 0 and molecule 1, Asp1 and Asp2, respectively. Due to their symmetry, a torsion of the side chains by 180 degrees (four steps) results in the initial state and is hence treated as zero rotation. For the same reason, a (backward) rotation of three steps corresponds to a (forward) rotation by one step.

Wi is the i^{th} water pattern of all thirteen water molecules. Different water patterns, that is different orientations of the water molecules, can be achieved by translation or rotation of a single or several water molecules, discretised in displacement steps of 2 Å for translation and 22.5° for rotation, respectively. The complete labelling of a water pattern consists of 78 digits in total. These are three digits for the number of translation steps in x, y, and z-direction, respectively, and three digits for the rotation steps around the three principal axes, respectively, for each water molecule (see Tab. S7 for complete water pattern labelling of the most important nodes). The index i is just used as a counter for a compact notation. Its value therefore does not quantify the distance between water patterns.

P indicates the protonation state given by the number of the molecule (see Fig. 2a) that carries the excess proton. In principle, states that differ from the reactant state by multiple protonations/deprotonations of one or more molecules can be envisaged but are not sampled in this work. The reactant state is labelled as 0.0.w0.0 corresponding to zero displacement along the side chain dihedral angles of molecule 0 and 1, respectively, zero displacement of all water molecules, and location of the excess proton at molecule 0 (Asp1). A node labelled 0.2.w231.3 (SC0=0.SC1=2.Wi=W231.P=3) signifies the following displacement with respect to the reactant state: zero rotation around the side chain of molecule 0 (Asp1), two rotation steps (2·45°) around side chain dihedral angle of molecule 1 (Asp2), water pattern number 231 (see Tab. S7), and the excess proton is located on molecule 3 (a water molecule, see Fig. 2a) .

Transitions between selected pairs of nodes v_i and v_k were computed as minimum energy pathways, using the conjugate peak refinement [47] as implemented in CHARMM [48]. The transition between two nodes represents an edge of the transition network. A minimum energy pathway between two states

(nodes) can lead via several transition and intermediate states. The transition state with the highest energy is, according to transition state theory, the rate-determining one and its relative energy is thus used as the edge weight, i.e. the cost for going from node v_i to node v_k along that edge.

Two nodes were selected to form a pair if they differ by at most one step per degree of freedom sampled: one dihedral step, the proton position, the position of the proton-carrying water molecule in the additional control, and the displacements of the water molecules (a single translation of (2 Å in either x, y, or z-direction, respectively, and a single rotation of 22.5° around the three principal axes, respectively) in the full sampling.

All nodes connected by edges were combined to form the transition network. For finding the pathway that optimises the transition time between reactant and product states, the path that minimises the sum of all transition times needs to be determined. The transition time between two nodes, v_i, v_k , can be regarded as proportional to $w_{i,k} = \exp\left[\frac{E_{i,k}}{k_B T}\right]$ where $E_{i,k}$ is the energy of the transition state between the two nodes, k_B is Boltzmann’s constant and T is the temperature. Using $w_{i,k}$ as an edge weight, the cost of a path on the transition graph $P(v_1, \dots, v_n)$ where v_j are the nodes, is the sum of all edge weights along that path $C(P) = \sum_{j=1}^n w_{j,j+1}$. Because of the exponential weighting, this sum is dominated by the highest transition state energy [40].

The “best path” is thus the energetically most favourable pathway between reactant and product, i.e. the path with the lowest maximal (highest transition state) energy along that path. We therefore use the term “best path” rather than shortest path in the following. This best path was determined using Dijkstra’s algorithm [49].

In addition, all next best pathways within an energy range, were computed using the same algorithm as in Ref. [40].

All simulations were performed using the CHARMM program [48]. QM-optimisations of stationary points have been performed using CHARMM, interfaced to MNDO [50]. Direct generation of configurations, node assignment, determination of neighbour pairs, compilation and analysis of the network were carried out using our own java code and java libraries provided by Noe *et al* [40].

2. Results and Discussion

2.1. Transition Network from direct sampling

Direct sampling of side chain rotations and excess proton positions generates 1088 initial states of which, after minimisation, 206 different nodes result. Between those nodes 4193 neighbour pairs were identified and the corresponding edges computed to construct a transition network. Product and reactant state are energetically equal since they are chemically equivalent states with the excess proton located at one of the two aspartate mimics, respectively. The best paths have a highest barrier of 5 kcal/mol. Five pathways with a rate-determining barrier of that height can be identified in the transition network. Fig. 3 shows

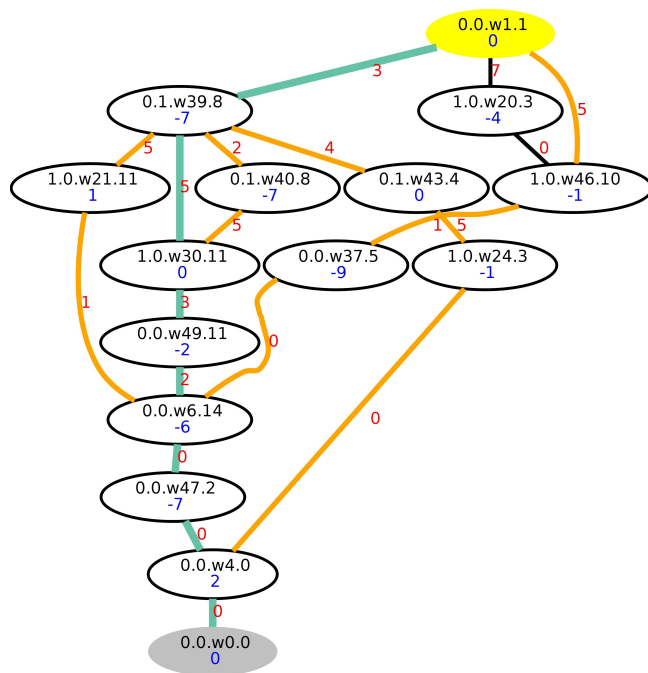


Figure 3: Proton transfer transition network from direct sampling of side chain rotations and protonation states, TN-direct. The nodes are shown as ellipses, labelled after the full set of degrees of freedom used: side chains, water pattern, and proton positions (SC0.SC1.Wi.P). The ellipses filled in grey and yellow colour correspond to the reactant and product state, respectively. Edges are shown as lines connecting two nodes. Blue numbers are energies of the respective node, red numbers are the energies of the highest transition state along that edge used as edge weights. All energies are in kcal/mol and relative to the reactant state, rounded to integer values for better readability. The best path is highlighted in turquoise, the next best paths are shown in orange.

the best path and all next best paths up to a rate-determining barrier, i.e. the highest barrier along the path, of 7 kcal/mol. All best pathways go through a state with SC0.SC1=1.0 for the side chains, i.e. require at least one side chain rotation along the pathway. All, but one, best pathways shown in Fig. 3, also show a rotation of the other side chain (labelled as 0.1). Furthermore, all steps of all best pathways in this transition network (TN-direct) are associated with a change in the water pattern, i.e. at least one water molecule undergoes a rotational or translational transition.

2.2. Transition network from combined sampling

For construction of the transition network presented in Fig. 4, all (7462) different nodes obtained from the MD simulations and those from the direct sampling of side chains and proton positions were combined and connected by 134527 edges in total. 47468 of those edges are connections of nodes that are generated by the MD sampling. The best pathway in this transition network

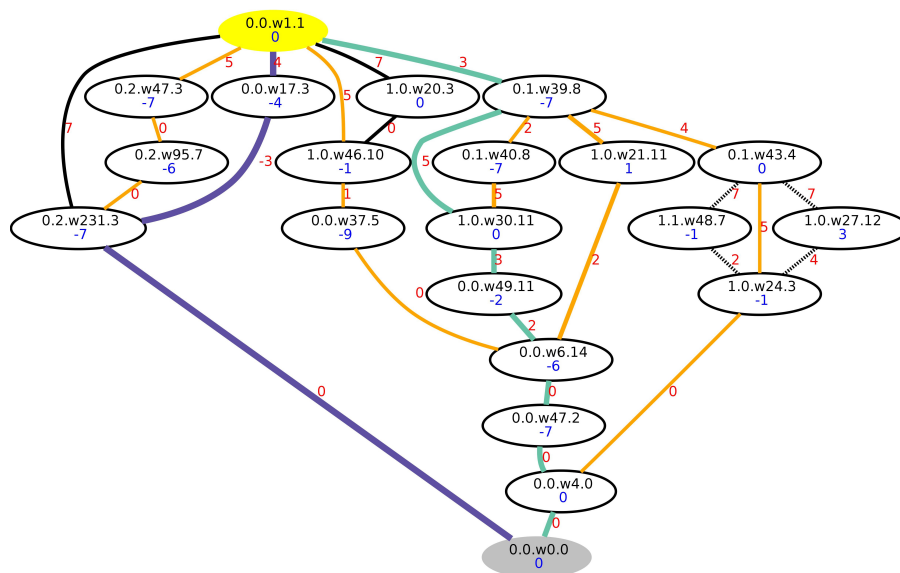


Figure 4: Proton transfer transition network from full set of states, direct sampling of side chain rotations, protonation states combined with sampling of water molecule positions and orientations by MD simulations, TN-combined. The nodes are shown as ellipses, labelled after the full set of degrees of freedom used: side chains, water pattern, and proton positions (SC0.SC1.Wi.P). The ellipses filled in grey and yellow colour correspond to the reactant and product state, respectively. Edges are shown as lines connecting two nodes. Blue numbers are energies of the respective node, red numbers are the energies of the highest transition state along that edge used as edge weights. All energies are in kcal/mol and relative to the reactant state, rounded to integer values for better readability. The best path is highlighted in indigo, the next best paths are shown in orange. The pathway drawn in turquoise has the same highest barrier as those coloured in orange. It is, however, emphasised because it is the same pathway as the best pathway in the transition network from direct sampling (TN-direct, Fig. 3). The dashed lines indicate edges and resulting pathways that are additional to the transition network constructed from direct sampling of side chain rotations, protonation states and positions of the proton-carrying water molecules.

has a highest barrier of 4 kcal/mol and consists of only three steps for which changes in all degrees of freedom are required, except for torsion of the first aspartate mimic. One of the second best pathways with a highest barrier of 5 kcal/mol (coloured in turquoise in Fig. 4) is the same as the best pathway in the transition network obtained from only direct sampling (TN-direct), indicating that the positions of water molecules, with or without excess proton, are at least partially adjusted in the minimisation procedure. However, those nodes passed by the best pathway in the combined transition network would be missed if water positions and orientations were not sampled.

The structures of the nodes along the best and second best pathway (i.e. the best pathway in TN-direct) are shown in Fig. 5. In both, best and second best pathways, in all intermediates an Eigen-ion or Eigen-like ion is formed that contains the excess proton. Along the best path, the initial step is a proton transfer to the water molecule next to the initially protonated aspartate mimic, associated with a reorientation of the two water molecules that are hydrogen-bonded to the proton accepting water molecule. Also the second aspartate mimic rotates. Then, a small, further reorientation of another water molecule and again the second aspartate mimic takes place before the final concerted proton transfer step via three hydrogen bonds that leads to the product state. These subtle changes which enable the final transition over the highest barrier of this best pathway are those which are obtained by the additional sampling of water positions and orientations only. The pre-orientation of the aspartate side chains and hydrogen-bonded water molecules can be understood as taking place in the resting state prior to the actual proton transfer step in the active state.

The second best pathway starts with a reorientation of all the water molecules, followed by three single proton transfer steps, all of which associated with reorientation of the proton-donating or accepting water molecules and one or two additional water molecules that are hydrogen-bonded to them. In the last three steps, during which the excess proton is already located at the water molecule that is hydrogen-bonded to the second aspartate mimic, further such water reorientation takes place. However, it is now the torsion of the first, and then both aspartate mimics that precede the final proton transfer to the product state.

Interestingly, this whole second best pathway is contained in the transition network obtained from direct sampling only, including the first intermediate state that differs from the reactant state by water reorientation. Since water reorientation has not been sampled in the TN-direct, this state is a consequence of the minimisation leading away from the initial sample. It is therefore important that the node assignment procedure considers also degrees of freedom that are not followed in the initial, direct sampling. In the current example, this would have been of no consequence, as the edge to and from the node 0.0.w.0 and the node itself, all have the same energy as the reactant state. In other, especially in more complex systems, this may not be the case.

We generated another transition network by direct sampling of the proton-carrying water positions, in addition to the direct sampling of side chain ro-

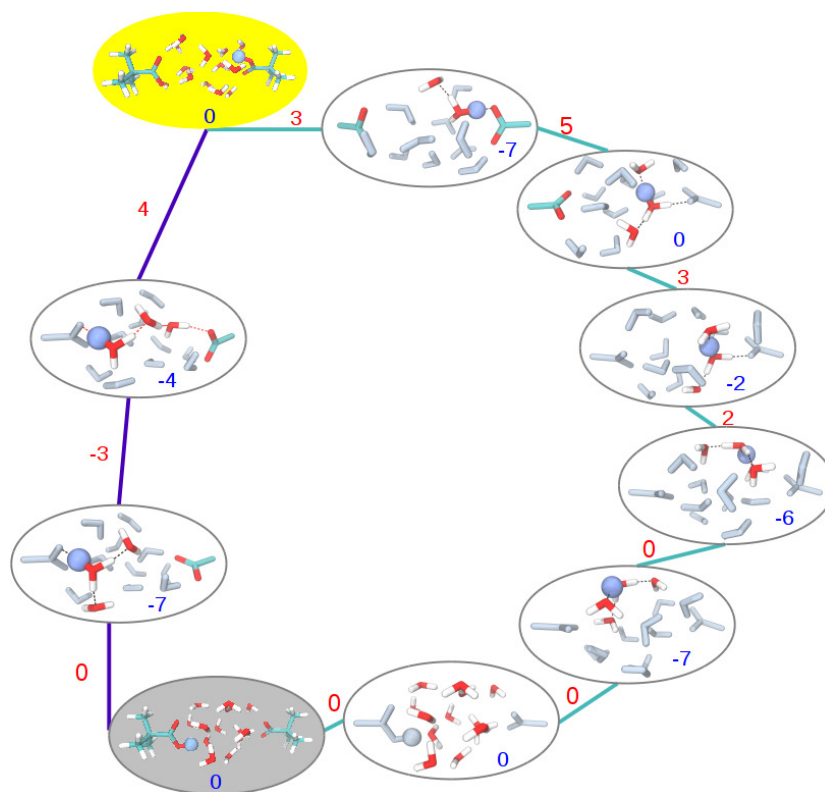


Figure 5: Structures of the nodes, intermediate states and end states, along the two best paths as computed in the transition network shown in Fig. 4. Blue numbers are energies of the respective node, red numbers are the energies of the highest transition state along that edge used as edge weights. All energies are in kcal/mol and relative to the reactant state, rounded to integer values for better readability. The best path is highlighted in indigo, the second best path in turquoise, respectively. For clarity, the bulky ends of the aspartate mimics are not shown in the intermediate states. The part of the system that changes with respect to the previous state is highlighted in colour. Blue spheres are protons to be transferred or just transferred. Coloured water molecules indicate their change in position and/or orientation, coloured side chains indicate a torsional transition.

tations and proton positions, in order to check how well this reproduces the best pathways from the combined direct and MD-based sampling. The further sampling of some water positions leads to 6080 initial states of which 1230 nodes remain. The resulting transition network consists of 42692 edges. In fact, comparing only the pathways up to a rate-determining barrier of 7 kcal/mol it almost completely reproduces the transition network from the combined sampling, except for two pathways, indicated by dashed lines in Fig. 4.

Tab. 1 lists the number of best paths up to a highest barrier energy of 10 kcal/mol for all three transition networks calculated. The number of additional best pathways, compared to those obtained by only direct sampling, grows considerably, when including more different nodes as provided by the additional MD-based sampling. Pathways with similar rate-determining barriers within the error of the electronic structure method used for the calculation of minima and transition states should be considered as energetically equivalent. The semi-empirical calculations performed in this work are estimated (see supplementary material) to have an error of up to ± 4 kcal/mol with respect to density functional theory calculations.

The transition network approach allows to identify these energetically similar pathways which can, however, differ remarkably in the structural changes of the states visited along those pathways. According to earlier suggestions [33] proton transfer follows a combination of proton “hops” and concerted proton transfer along water-wires. The best pathway identified in this work is in agreement with this suggestion. The second best pathway, however, exhibits only step-wise transitions, similar to the pure “Grotthus” mechanism observed in earlier simulations of other hydrogen-bonded networks [22]. Both these two pathways are very close in energy and yet can be assigned to different categories. The sampling approach employed in this work does not suffer from pre-selected reaction coordinates and hence enables the identification of such mechanistically different pathways.

The structural diversity of proton transfer pathways with comparable probability highlights the complexity of this type of reactions which cannot be described by a single mechanism. Even more complex systems such as proteins offer a vast variety of energetically similar, but structurally diverse, proton transfer pathways which are all conceivable to be employed and should therefore be included in a mechanistic study.

3. Conclusions

Our combined approach of direct sampling with an MD-based sampling provides a comprehensive and efficient way to capture all degrees of freedom that are relevant in the proton transfer process. The best pathways determined in the transition networks constructed from this combined sampling show an interplay of all these different degrees of freedom. In the energetically most favourable pathway, the pre-orientation of a hydrogen-bonded chain facilitates the concerted proton transfer to the product state. The second best pathway is

Table 1: Number of best paths within a given energy range for the transition networks generated by direct sampling of proton positions (TN-direct), direct sampling of proton and proton-carrying water positions (TN-direct-plus), and combination of direct sampling with MD-based sampling (TN-combined).

Barrier kcal/mol	Number of pathways		
	TN-direct	TN-direct-plus	TN-combined
1	0	0	0
2	0	0	0
3	0	0	0
4	0	1	1
5	5	6	6
6	0	0	0
7	1	2	4
8	3	9	11
9	2	7	10
10	1	9	10
up to 10	12	34	42

a step-wise proton transfer which is also found as the best pathway in the transition network from direct sampling. In addition to these two best pathways, the transition network allows to identify several other pathways with highest barriers of similar energy among which many are not contained in a transition network obtained from only the direct sampling. Identification of ensembles of pathways will be even more important in complex systems with a huge variety of energetically feasible, yet mechanistically diverse, reaction pathways.

Combined transition networks are an efficient way to capture this complexity and variability of proton transfer reactions.

Acknowledgement

We thank the Deutsche Forschungsgemeinschaft (DFG) for financial support provided to the Sonderforschungsbereich SFB 1078 on 'Protonation Dynamics in Protein Function'. HPC support in the physics department of the Freie Universität Berlin is gratefully acknowledged. We are grateful to Frank Noe for making the sources of his Transition Networks implementation for conformational transitions and other useful libraries such as MolTools available to us.

References

- [1] J. K. Lanyi, Bacteriorhodopsin, *Annu. Rev. Physiol.* 66 (2004) 665–688.
- [2] P. Mitchell, Chemiosmotic coupling in oxidative and photosynthetic phosphorylation., *Biol. Rev.* 41 (1966) 445–502.
- [3] H. J. Morowitz, Proton semiconductors and energy transduction in biological-systems, *Am. J. Physiol.* 235 (1978) R99–114.
- [4] W. Rüttinger, G. C. Dismukes, Synthetic water-oxidation catalysts for artificial photosynthetic water oxidation, *Chem. Rev.* 97 (1) (1997) 1–24.
- [5] J. S. Vrettos, J. Limburg, G. W. Brudvig, Mechanism of photosynthetic water oxidation: combining biophysical studies of photosystem II with inorganic model chemistry, *Biochim. Biophys. Acta (BBA) - Bioenergetics* 1503 (2001) 229–245.
- [6] D. Walz, S. R. Caplan, Bacterial flagellar motor and h^+ /atp synthase: two proton-driven rotary molecular devices with different functions., *Bioelectrochemistry* 55 (2002) 89–92.
- [7] M. Capasso, T. E. DeCoursey, M. J. S. Dryer, pH regulation and beyond: unanticipated functions for the voltage-gated proton channel, *hvcn1*, *Trends Cell Biol.* 21 (2011) 20–28.
- [8] D. Bustah, G. Szabo, Gramicidin forms multi-state rectifying channels, *Nature* 294 (1981) 371–373.
- [9] K. Kreuer, S. J. Paddison, E. Spohr, M. Schuster, Transport in proton conductors for fuel-cell applications: Simulations, elementary reactions, and phenomenology, *Chem. Rev.* 104 (2004) 4637–4678.
- [10] P. Meredith, C. J. Bettinger, M. I.-V. M. A. B. Mostert, P. E. Schwenn, Electronic and optoelectronic materials and devices inspired by nature, *Rep. Prog. Phys. Soc.* 76 (2013) 034501.
- [11] C. J. T. V. Grotthuss, Sur la decomposition de l'eau et des corps qu'elle tient en dissolution a l'aide de l'electricite galvanique (theory of decomposition of liquids by electric currents), *Ann. Chim.* 58 (1806) 54–74.
- [12] J. D. Bernal, R. H. Fowler, A theory of water and ionic solution, with particular reference to hydrogen and hydroxyl ions, *J. Chem. Phys.* 1 (1933) 515–548.
- [13] M. Eigen, L. de Maeyer, Self-dissociation and protonic charge transport in water and ice, *Proc. Roy. Soc. (London)* 247 (1958) 505.
- [14] M. Tuckerman, K. Laasonen, M. Sprik, M. Parrinello, Ab initio molecular dynamics simulation of the solvation and transport of hydronium and hydroxyl ions in water., *J. Chem. Phys.* 103 (1995) 150–161.

- [15] D. Marx, M. E. Tuckerman, J. Hutter, M. Parrinello, The nature of the hydrated excess proton in water., *Nature* 397 (1999) 601–604.
- [16] P. Geissler, C. Dellago, D. Chandler, J. Hutter, M. Parrinello, Autoionization in liquid water, *Science* 291 (2001) 2121–2124.
- [17] C. Knight, G. A. Voth, The curious case of the hydrated proton., *Acc. Chem. Res.* 45 (2012) 101–109.
- [18] G. A. Voth, Computer simulation of proton solvation and transport in aqueous and biomolecular systems, *Acc. Chem. Res.* 39 (2006) 143–150.
- [19] C. Knight, C. M. Maupin, S. Izvekov, G. A. Voth, Defining condensed phase reactive force fields from ab-initio molecular dynamics simulations: the case of the hydrated excess proton., *J. Chem. Theory. Comput.* 6 (2010) 3223–3232.
- [20] O. Markovitch, H. Chen, S. Izvekov, F. P. G. A. Voth, N. Agmon, Special pair dance and partner selection: elementary steps in proton transport in liquid water., *J. Phys. Chem. B* 7 (2008) 9456–9466.
- [21] N. Agmon, The grotthuss mechanism, *Chem. Phys. Lett.* 244 (1995) 456–462.
- [22] D. Marx, Proton transfer 200 years after von grotthuss: Insights from ab initio simulations, *Chem. Phys. Chem.* 8 (2007) 209–210.
- [23] L. Onsager, The motion of ions: principles and concepts, *Science* 166 (1969) 1359–1364.
- [24] M. Eigen, proton transfer, acid-base catalysis, and enzymatic hydrolysis. part i: Elementary processes., *Angew. Chem. Int. Ed. Engl.* 3 (1964) 1–19.
- [25] J. F. Nagle, M. Mlle, H. J. Morowitz, Theory of hydrogen-bonded chains in bioenergetics., *Biophys. J.* 25 (1979) 3959.
- [26] Q. Cui, M. Karplus, Is a proton wire concerted or stepwise? a model study of proton transfer in carbonic anhydrase., *J. Phys. Chem. B.* 107 (2003) 1071–1078.
- [27] C. Dellago, M. M. Naor, G. Hummer, Proton transport through water-filled carbon nanotubes, *Phys. Rev. Lett.* 90 (2003) 105902.
- [28] S. Izvekov, G. A. Voth, Ab initio molecular-dynamics simulation of aqueous proton solvation and transport revisited., *J. Chem. Phys.* 123 (2005) 044505.
- [29] R. L. A. Timmer, M. J. Cox, H. J. Bakker, Direct observation of proton transfer in ice ih using femtosecond spectroscopy., *J. Phys. Chem. A* 114 (2010) 2091–2101.

- [30] M. J. Cox, R. L. Timmer, H. J. Bakker, S. Park, N. Agmon, Distance-dependent proton transfer along water wires connecting acid-base pairs., *J. Phys. Chem. A* 113 (2009) 6599–6606.
- [31] R. Shevchuk, N. Agmon, F. Rao, Network analysis of proton transfer in liquid water, *J. Chem. Phys.* 140 (2014) 244502.
- [32] A. Hassanali, M. Krakash, H. Eshet, M. Parrinello, On the recombination of hydronium and hydroxide ions in water, *Proc. Natl. Acad. Sci. USA* 108 (2011) 20410–20415.
- [33] A. Hassanali, F. Giberti, J. Cuny, T. D. Kuehne, M. Parrinello, Proton transfer through the water gossamer, *Proc. Natl. Acad. Sci. USA* 110 (2013) 13723–13728.
- [34] M. A. Lill, V. Helms, Molecular dynamics simulation of proton transport with quantum mechanically derived proton hopping rates (q-hop md), *J. Chem. Phys.* 115 (2001) 7993–8005.
- [35] R. Vuilleumier, D. Borgis, An extended empirical valence bond model for describing proton transfer in $\text{h}^+(\text{h}_2\text{o})_n$ clusters and liquid water, *Chem. Phys. Lett.* 284 (1998) 71–77.
- [36] U. W. Schmitt, G. A. Voth, Multistate empirical valence bond model for proton transport in water, *J. Phys. Chem. B* 102 (29) (1998) 5547–5551.
- [37] S. Pezeshki, H. Lin, Adaptive-partitioning qm/mm for molecular dynamics simulations: 4. proton hopping in bulk water, *J. Chem. Theor. Comput.* 11 (6) (2015) 2398–2411.
- [38] D. J. Wales, Discrete path sampling, *Molecular Physics* 100 (20) (2002) 3285–3305.
- [39] D. J. Wales, Energy landscapes: calculating pathways and rates, *International Reviews in Physical Chemistry* 25 (1-2) (2006) 237–282.
- [40] F. Noé, D. Krachtus, J. C. Smith, S. Fischer, Transition networks for the comprehensive characterization of complex conformational change in proteins, *J. Chem. Theory Comput.* 2 (2006) 840–857.
- [41] H. Ishikata, K. Saito, Proton transfer reactions and hydrogen bond networks in protein environments, *J. R. Soc Interface.* 11 (2014) 20130518.
- [42] M. I. Verkhovskiy, A. Jasaitis, M. L. Verkhovskaya, J. E. Morgan, M. Wikström, Proton translocation by cytochrome c oxidase, *Nature* 400 (6743) (1999) 480–483.
- [43] V. Sharma, M. Wikström, V. R. Kaila, Dynamic water networks in cytochrome cbb 3 oxidase, *Biochimica et Biophysica Acta (BBA)-Bioenergetics* 1817 (5) (2012) 726–734.

- [44] D. G. Levitt, S. R. Elias, J. M. Hautman, Number of water molecules coupled to the transport of sodium, potassium and hydrogen ions via gramicidin, nonactin or valinomycin., *Biochim. Biophys. Acta* 512 (1978) 43–6451.
- [45] D. Sagnella, G. Voth, Structure and dynamics of hydronium in the ion channel gramicidin a, *Biophysical Journal* 70 (1996) 2043 – 2051.
- [46] W. Thiel, W. Weber, Orthogonalizaion corrections for semiempirical methods., *Theor. Chem. Acc.* 103 (2000) 495.
- [47] S. Fischer, M. Karplus, Conjugate peak refinement: an algorithm for finding reaction paths and accurate transition states in systems with many degrees of freedom, *Chem. Phys. Lett.* 194 (1992) 252–261.
- [48] B. R. Brooks, R. E. Bruccoleri, B. D. Olafson, D. J. States, S. Swaminathan, M. Karplus, CHARMM: A program for macromolecular energy, minimization and dynamics calculations, *J. Comp. Chem.* 4 (1983) 187–217.
- [49] E. A. Dijkstra, A note on two problems in connection with graphs., *Num. Math.* 1 (1959) 269.
- [50] W. Thiel, MNDO Version 6.1, Max-Planck-Institut fuer Kohlenforschung, Mülheim a.d.Ruhr, Germany (2004).